Optical Materials 152 (2024) 115396

Contents lists available at ScienceDirect

Optical Materials

journal homepage: www.elsevier.com/locate/optmat

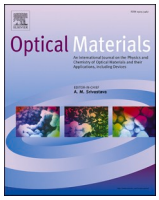

Research Article

A new strategy to prepare high luminescent films containing polypropylene and polyamide doped with Eu^{3+} β-diketonate complex

D.F. Parra [a,*], L.G. Marchini [a], M.C.F.C. Felinto [a], H.F. Brito [b]

[a] Chemical and Environmental Center – Nuclear and Energy Research Institute, IPEN/CNEN, BR-05508-000, Sao Paulo, SP, Brazil
[b] Department of Fundamental Chemistry, Institute of Chemistry, University of Sao Paulo, BR-05508-000, Sao Paulo, SP, Brazil

ARTICLE INFO

Keywords:
Polyamide
Polypropylene
Polymer
Europium
β
Diketonate
Luminescence

ABSTRACT

A new strategy for obtaining stable luminescent polypropylene (PP) one polymer among the most consumed plastic materials is reported. PP is a polymer of nonpolar olefinic macrochains, preventing direct doping with rare earth complexes. The synthesis of the polyamide (PA) polymer doped with hydrated complex [Eu(tta)$_3$(H$_2$O)$_2$] and its encapsulation in PP polymer produced a luminescent material stable under processing conditions of the plastic films as never been seen before. The preparation of the Eu^{3+} β-diketonate complex and polyamide solution produced a high luminescent material. The processed polymeric films doped in different concentration fo the europium complex were characterized by infrared spectroscopy (FTIR), X-ray diffractometry (XRD), emission spectroscopy, and thermogravimetry (TG). The emission spectra of the luminescent doped polymeric films exhibited the characteristic narrow bands arising from the $^5D_0 \rightarrow {}^7F_J$ transitions (J = 0–4) of the Eu^{3+} ion. The values of the Ω_2 and Ω_4 experimental intensity parameters were calculated and discussed. The high values of the intrinsic emission quantum yields (Q_{Eu}^{Eu}) of the PA:[Eu(tta)$_3$(H$_2$O)$_2$] systems suggest that these films can be applied as optical markers as well as the encapsulated systems of the (PP) as PP/PA:(x%)Eu(tta)$_3$ films (x = 1, 5, and 10 %). The stability was promoted via PP encapsulation resulting in a luminescent plastic film with high stability under processing.

1. Introduction

Luminescent materials doped with lanthanide ions play essential roles in display technology, biomolecular sensors, luminescent markers, optical-electronic devices, as well as phosphors [1–3]. In the last decades, the optical study of the Ln^{3+} complexes with β-diketonate ligands was increased owing to the intrinsic spectroscopic properties [3]. These luminescent rare earth compounds behave as efficient light conversion molecular devices (LCMDs), where the organic ligands may act as efficient sensitizers for the light-emitting lanthanide ions through an intramolecular energy transfer process [4]. Usually, Ln^{3+} β-diketonate compounds present the *antenna effect* to denote a high efficiency in the sequence of ligand (L) absorption, intramolecular energy transfer (L→Ln^{3+}), and emission arising from the intraconfigurational 4f transitions of the metal ions [4–6].

Eu^{3+} ion is suitable for luminescent materials due to its characteristic narrow emission bands, resulting in a red emission color with a monochromatic character. Besides, the significant advantages are the large energy gap between the emitting level ($^5D_0$), and the ground states ^7F_J ($J = 0$ to 6) is at around 12000 cm^{-1}; long lifetimes of the emitter $^5D_0$ level (ms); and the large Stokes shift, among others [2,5,7].

Ln^{3+}-complexes doped in organic polymers have several significant gains as photosensitivity, mechanical integrity, corrosion protection, transparency, and suitable adhesion properties. Furthermore, the polymeric networks may encapsulate large amounts of emitting centers, isolated from each other, and protected by the organic host as well as for siloxane-based hybrid systems, generally, allowing a decrease of non-radiative processes [8–10].

The photoluminescence study of the Eu^{3+} complexes in polymeric matrices has been extensively developed [11–13]. These kinds of compounds were successfully loaded into the polystyrene nanoparticles enabling their bioanalytical application in the aqueous environment. The biodegradable polymer doped with Eu^{3+} complexes: poly (b–hydroxybutyrate):Eu(tta) (labeled as PHB:Eu(tta)) performed highly efficient luminescence for biodegradable optical markers [13]. Moreover, polystyrene (PS) latex nanoparticles doped with Eu^{3+} β-diketonate complexes can be used for luminescent dyes in related applications such as single-dye labeled oligonucleotides, or conjugation for cell and tissue

* Corresponding author.
E-mail address: dfparra@ipen.br (D.F. Parra).

https://doi.org/10.1016/j.optmat.2024.115396
Received 29 August 2023; Received in revised form 12 March 2024; Accepted 13 April 2024
Available online 29 April 2024
0925-3467/© 2024 Elsevier B.V. All rights reserved.

staining [14].

Besides, Eu^{3+} β-diketonate complexes have been embedded into polymethylmethacrylate (PMMA) polymer films, showing higher thermal stability and high intrinsic emission quantum yield as compared to the precursor lanthanide complex [15,16]. These results showed that the PMMA polymer with a high molecular weight enwraps the Eu^{3+} complex, which results in a high luminescence intensity due to the effective intermolecular energy transfer. Therefore, the PMMA films doped with the Eu^{3+} β-diketonate complexes showed promising PL efficiency [15,16].

Otherwise from these well-known doped polymers, the Eu^{3+} β-diketonate complexes doped in polyolefins have the disadvantage of no coordination with their polymeric macrochains. The chemical feature of polyolefins is due to the absence of the oxygen atom (hard base) to bond to the Eu^{3+} ion (hard acid) to replace the water molecules of the complex. Although polypropylene (PP) is non-reactive, it is possible to embed with the poly-ε-caproamide (PA) polymer (Fig. 1) doped with Eu^{3+} complex.

In this work, we report the synthesis, characterization, thermal stability, and luminescent properties of polyamide, poly-ε-caproamide (PA) polymer films doped with the $[Eu(tta)_3(H_2O)_2]$ hydrated complex, (PA:(x%)$Eu(tta)_3$) at percentage ratio of x = 1, 5, and 10 %, in mass. The optical properties of the PA:(x%)$Eu(tta)_3$ luminescent materials and the tagged polypropylene (PP) polyolefin films have been discussed. Besides, it is observed that the mechanical processing of these composite materials in an extrusion process maintains their luminescent properties arising from the Eu^{3+} complex.

2. Experimental

2.1. Material preparation

The Eu^{3+} chloride was synthesized according to the literature [14] by the reaction of the europium oxide (Eu_2O_3) with concentrated HCl (37 % v/v). Subsequently, the $EuCl_3 \bullet 6H_2O$ in aqueous solution was filtered, and the solvent evaporated, leading to a crystalline solid that was dried and stored under reduced pressure.

The $[Eu(tta)_3(H_2O)_2]$ hydrated complex was prepared according to reference [16,17] by reacting the $EuCl_3 \bullet 6H_2O$ with HTTA. The molar ratio between the reactants was in the proportion 1:3 mols. The $EuCl_3 \bullet 6H_2O$ was dissolved in water and Htta was dissolved in alcohol. The alcoholic solution of Htta had a pH controlled to 6.5 with ammonium hydroxide solution 6 Mol. The solutions were put together and were heated to 60°C for an hour until precipitate formation. The yellowish precipitate formed was separated from the solution by filtration and was purified by washing than with water, and dried under reduced pressure in a vacuum desiccator (Yield: 90 %). The C, and H contents for controlling were determined by elemental analysis in a CHN 2400 (PerkinElmer) analyzer.

The polymeric films were prepared by dissolving the polyamide (PA) in formic acid (1 N) followed by the addition of the required amount of the Eu^{3+}-complex. The polyamide (PA) polymer was doped with the $[Eu(tta)_3(H_2O)_2]$ complex in the rations of 1, 5, and 10 % (w/w). The polyamide (PA) polymer used in this work, was supplied in powder form by BASF (São Paulo-SP, Brazil) and had a molecular weight of repeat unit: 113.16 g mol^{-1}, and averaged molecular weight (M_w) of 48000 g mol^{-1}, with PA accounting for 99.9 % of the dry material.

The PA powder (0.2 g) was dissolved in formic acid 1 N, (50 mL) followed by the addition of the required amount (from 1 to 10 % in mass) of the Eu^{3+}−complex in acetone solution. The mixed solution was heated at 40 °C for 30 min and then casted onto a Petri dish. The polymer film was obtained after the total evaporation of the solvent at 60 °C.

To obtain the luminescent PP pellets, the PP polymer, isotactic polypropylene (PP) pellets supplied by Braskem, with a Melt Flow Index of 3.5 dg mol^{-1}, density of 0.905 g cm^{-3}, and M_w = 300,000 g mol^{-1} was processed by extrusion. The material extruded of the doping PA:$Eu(tta)_3$ in PP follows the procedure: 300 g of PP were mixed in a beaker with 3 g (10%w/w) of the PA:x% $Eu(tta)_3$, (x:1, 5, 10 %) each one previous and manually sectioned. The mixtures were extruded in a Haake Polylab OS extruder. This extruder having double screw and heating temperature zones of 190, 195, 198, 200, 205 and 210 °C operated with a screw rotation speed of 100 rpm.

2.2. Characterization

The elemental analyses were performed in PerkinElmer CHN 2400 instruments. X-ray diffraction patterns were registered on an X-ray diffractometer with a source of $CuK_{\alpha 1}$ radiation (λ = 1.54056 Å) generated at 30 kV and 20 mA. The angle (2θ) range was from 5 to 80° with a pitch of 0.05°, and an acquisition time of 1s in the Rigaku Mine Flex II apparatus. The identification of the crystalline phase was obtained with the aid of the software program PDXL Software. Thermogravimetric analyses (TG) were achieved with a TG/SDTA 822 thermobalance (Mettler-Toledo), using alumina crucibles containing around 10 mg of the sample, under dynamic $N_{2(g)}$ or $O_{2(g)}$ oxygen atmospheres (50 mL·min^{-1}) at a heating rate of 10°C·min^{-1}. Infrared absorption spectra of the samples were recorded using KBr pellets with a Bomem MB102 FTIR spectrometer in the range from 400 to 4000 cm^{-1} with a spectral resolution of 4.0 cm^{-1}.

Excitation and emission spectra were obtained at room temperature, 298 K, in a SPEX-Fluorolog-3 (Horiba FL3-22iHR320) spectrofluorimeter with double grating between 0.5 and 2.0 mm monochromator (SPEX1680), and the excitation source was a 450 W Xenon lamp. Excitation spectra were obtained in the range from 250 to 500 nm, and emission spectra from 550 to 720 nm. Emission decay curves were obtained using a pulsed Xenon lamp of 150 W up to 11 ms. The emission and excitation slits were used with opening between 0.3 and 1 nm. All spectral data were collected at an angle of 22.5° (front face). The emission spectra were obtained by monitoring excitation at $\lambda_{ex.}$ = 350 nm, corresponding to the absorption of the S→S_0 transition of the organic part. All measurements of spectrophotometry were obtained in the equipment belonging to the Multiuser Laboratory of Advanced Optical Spectroscopy - LMEOA, of the Chemistry Institute of UNICAMP - Campinas, São Paulo.

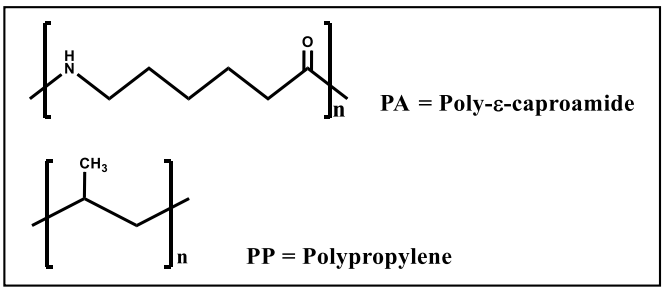

Fig. 1. Molecular structures of polypropylene (PP) and poly-ε -caproamide (PA) polymers.

3. Results and discussion

The founded and calculated elemental analysis data (%) of the Eu complex showed good agreement between each other, *i.e.*, $EuO_8C_{24}H_{16}F_9S_3$: found. calc.: C = 33.85 %; H = 1.89 % and found C = 33.91 %; H = 1.93 % that refers the formula of $[Eu(tta)_3(H_2O)_2]$. This result suggests the formation of a hydrated complex $[Eu(tta)_3(H_2O)_2]$.

The TG curve of the $[Eu(tta)_3(H_2O)_2]$ complex shows one first event in temperature interval from 30 to 120 °C attributed to the mass loss of the two water molecules in the first coordination sphere. In addition, the second thermal decomposition event from 120 to 360 °C was assigned to

tta ligands degradation (Fig. 2a). The PA:(10 %)Eu(tta) film showed one event at 275–310 °C attributed to the excess of the complex dispersed on the polymer PA (Fig. 2b). Otherwise, the TG curves of the polyamide (PA), polypropylene (PP) polymers as well as PA:(x%)$Eu(tta)_3$ and PP/PA:(x%)$Eu(tta)_3$ doped samples (x = 1 and 5 %) show the similar thermal decomposition profiles within only one event, starting at a temperature at around 412 °C, (Fig. 2c–e and Figs. S1 and S2).

The decomposition onset temperature (T_{onset}) value of the [Eu$(tta)_3(H_2O)_2$] complex in PA:(10 %)$Eu(tta)_3$ doped polymeric film increase from 219 to 279 °C, indicating the higher thermal stability of the complex in the polymer matrix (Table 1). Besides, it is also observed that increasing the concentration of Eu^{3+} complex in the polymer matrix, the values of T_{onset} slightly decrease for the doped materials (Table 1). This thermal behavior is quite similar to the thermal decomposition in the PHB:Eu(tta) system reported in Ref. [18]. In general, the encapsulation indicates that the luminescent Eu^{3+}-complex becomes more thermally stable due to the protection originating from both doped PA and PP/PA polymeric systems.

Also, TG curves of doped polymeric systems, recorded in the temperature interval from 25 to 200 °C, show the absence of loss mass (Fig. 2b–d, and Figs. S1c and d), which confirms that water molecules of the hydrated precursor complex are exchanged by the oxygen of PA polymer, after the doping reaction process. These data are consistent with the literature work [19] that reported the [Eu$(tta)_3(H_2O)_2$] complex doped into epoxy resin polymer.

The calorimetric data of all samples calculated from differential scanning calorimetry (DSC) curves of undoped and doped PA polymers (Table 1) present one slight decrease at ~6 °C, (T_{melt} ~ 216–220 °C) of pure PA polymer and PA:(x%)$Eu(tta)_3$ doped films. However, the T_{melt} values of the extruded PP/PA:(x%)$Eu(tta)_3$ system (~182 °C) do not change with the doping, suggesting that the melting temperature of the PP polymer system is more favorable for the extrusion process conditions than that of doped PA polymer, which is more economically viable. Moreover, concerning the results of loss mass in TG data of the PA:5 % $Eu(tta)_3$ and PA:10 % $Eu(tta)_3$ materials (Fig. 2 and Fig. S1 e S2), a new event was observed at ~250 °C, owing to organic ligand loss mass. It can corroborate that there was a saturation of the complex in PA at those concentrations in which the remaining complex is lost by thermal decomposition at 250 °C.

FTIR spectral data of the [Eu$(tta)_3(H_2O)_2$] complex, PA polymer, and PA:(x%)$Eu(tta)_3$ doped films are shown in (Fig. 3 and Table S1). The complex shows bands assigned to the ν_s and ν_{as} OH at 3590–3100 cm^{-1} and H–*O*–H bending at 1602–1546 cm^{-1} from coordinated water molecules. Furthermore, characteristics absorption peaks at 1139 and 930 cm^{-1}, attributed to $\nu_{as}(CF_3)$ and ν(C═C + C═O) of the tta group, respectively, and also in 1411 cm^{-1} (ν C–O diketone), 1189 cm^{-1} (ν C–F tta ligand), and 782 cm^{-1} (ν C–S tta ligand) as expected. The displacement of the C═O stretching from 1680 cm^{-1} in the free ligand (tta) to 1605 cm^{-1} provides evidence that the metal ion is coordinated through the oxygen atom [13].

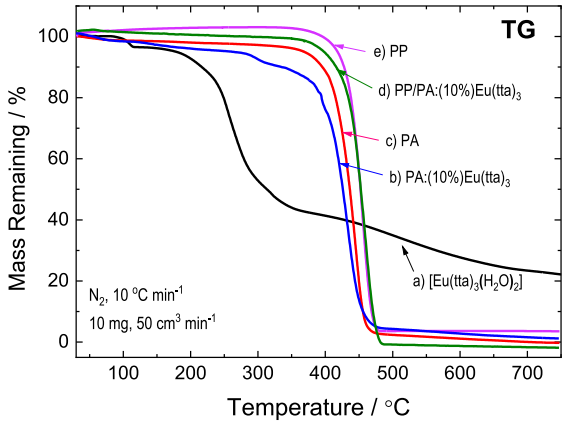

Fig. 2. TG curves of the materials: a) [Eu$(tta)_3(H_2O)_2$] complex (black line), b) PA:(10 %)$Eu(tta)_3$ (blue line), c) PA polymer (red line), d) PP/PA:(10 %)Eu$(tta)_3$ (green line)and e) PP polymer (violet line).

Table 1
The T_{onset} values of the PA:(x%)$Eu(tta)_3$ films and doped extruded PP/PA:(x%)$Eu(tta)_3$ PP polymer [Eu$(tta)_3(H_2O)_2$] precursor complex, in the extruded form PP/PA:5 % $Eu(tta)_3$ doped with 1, 5 and 10 % of complex [Eu $(tta)_3(H_2O)_2$]. DSC is the melting temperature (°C) and Integral (mJ) of the processed PP/PA:x% Eu $(tta)_3$ films doped with 1, 5, and 10 % of [Eu$(tta)_3(H_2O)_2$] complex.

Sample	T_{onset} TG (°C)		T_{melt} DSC (°C)
	tta	sample	sample
[Eu$(tta)_3(H_2O)_2$]*	229.0	–	–
PA	–	412.2	216.0
PA:(1 %)$Eu(tta)_3$	–	418.9	221.0
PA:(5 %)$Eu(tta)_3$	–	410.7	220.1
PA:(10 %)$Eu(tta)_3$	279.0	406.8	221.3
PP	–	435.9	183.4
PP/PA:(1 %)$Eu(tta)_3$	–	399.3	182.2
PP/PA:(5 %)$Eu(tta)_3$	–	430.6	181.8
PP/PA:(10 %)$Eu(tta)_3$	–	429.0	184.1
*coordinated waters	120.0 °C		

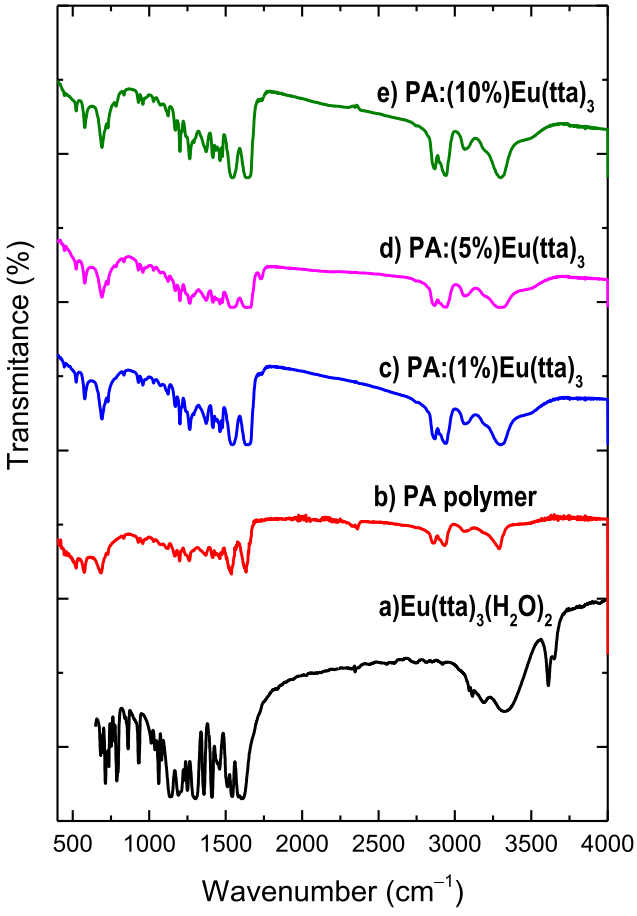

Fig. 3. FTIR absorption spectra of the: a) [Eu$(tta)_3.(H_2O)_2$], b) PA polymer, c) PA:(1 %)$Eu(tta)_3$, d) PA:(5 %)$Eu(tta)_3$ and e) PA:(10 %)$Eu(tta)_3$ in the range of 4000–400 cm^{-1}.

On the other hand, PA polymer spectra (Fig. 3 and Table S1) show the characteristic vibrations of the δN-H angular deformation and νCN stretch of amide in 1540, 1633, and 3290 cm^{-1} [20–22]. The bands in the region of 2859 and 2931 cm^{-1} are due to the stretching of $–CH_2$, $–CH_3$, and NH groups. A band at 1512 cm^{-1} is due to the N–H bending vibration of "free'' N–H groups and the bands in the region of 1200–900 cm^{-1} can be attributed to bending of the groups N–H, C–C–*O*–NH, and C═O of polyamide. For PA polymer doped Eu^{3+} complex, the stretching and deformation bands of the secondary amines, known as amide stretching I and II, are observed in 1641 cm^{-1} attributed to νC═O bonded and 1545 cm^{-1} attributed to $\delta_{N\text{-}H}$ bonded. The absorption peaks related to the H_2O vibrational modes of the $[Eu(tta)_3(H_2O)_2]$ are absent in the PA:(x%)Eu(tta) system. It is observed absorption band displacements of the non-doped PA doped polymers for the i) νC═O band from 1633 cm^{-1} to 1641 cm^{-1} and ii) the stretching δN-H from 1540 cm^{-1} to 1545 cm^{-1}. The absence of the N–H bending vibration of "free" N–H groups band in 1512 cm^{-1} in the doped material indicates the coordination between the PA – complex occurs replacing the coordination water molecules. It is worth noting that absorption bands assigned to the ν_s and ν_{as} OH in the range of 3590–3100 cm^{-1} and of δH-*O*-H bending at 1602–1546 cm^{-1} from coordinated water molecules in the complex are not present in the doped polymer (Fig. 3).

The X-ray diffraction patterns of undoped PA polymer at 20.2 and 23.7° are assigned to (200) and (202) planes of α-form crystals, respectively (Fig. 4). Also, the doped PA system with 1, 5, and 10 % of the Eu^{3+} complex shows the additional diffraction peaks at 16.8, 29.7, and 34° assigned to the Eu^{3+}-complex in the polymer system. The diffraction peaks (labeled as 1, 2, and 3) in PA:(x%)$Eu(tta)_3$ system (mainly at 10 %) also confirm the doping of the $[Eu(tta)_3{\cdot}(H_2O)_2]$ in the PA matrix and the increase of crystallinity in this system when the PA is doped with (Fig. 4), [23–25].

The undoped PP and doped PP/PA:(x%)$Eu(tta)_3$ systems present (Fig. S3, Table S2) five distinct diffraction peaks at 2θ around 13.9, 16.7, 18.3, 21.0, and 21.7° corresponding to the (110), (040), (130), (131) and (041) planes, respectively. These structural data are ascribed to the monoclinic α-crystalline phase of PP polymer from the crystallography point of view. Moreover, XRD patterns of the extruded PP/PA:(x%)Eu $(tta)_3$ samples (x = 1, 5, and 10 %) present only the diffraction peaks attributed to the phases concerning polypropylene considering the high concentration of PP polymer in the blends (Fig. S3).

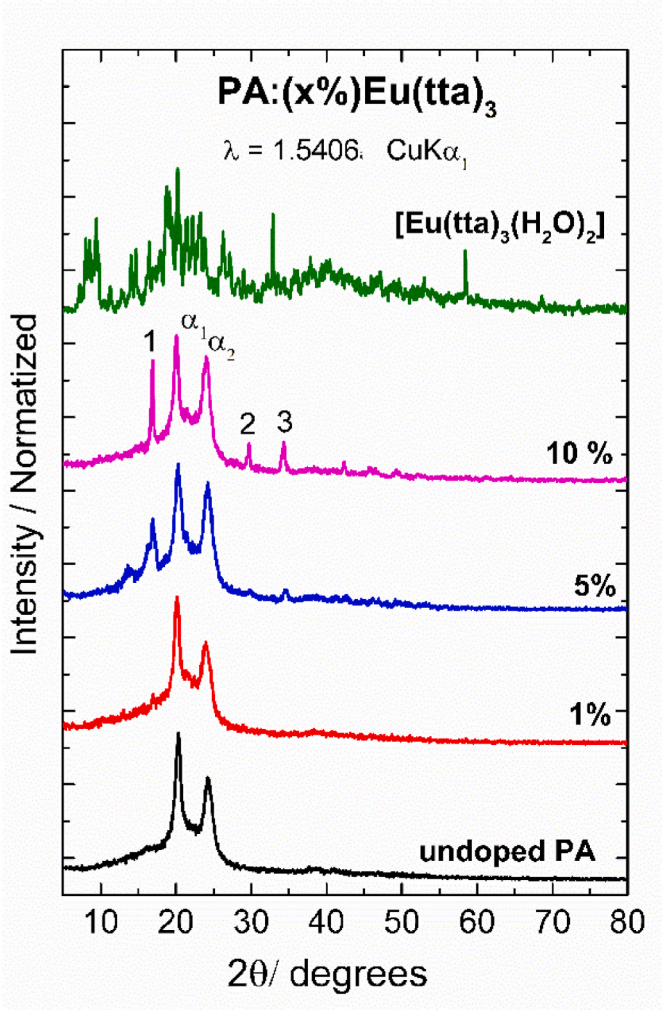

Fig. 4. The X-ray diffraction patterns of polymeric samples: undoped PA and doped PA:(x%)$Eu(tta)_3$ polymer films (x = 1, 5 and 10 %), and [Eu $(tta)_3(H_2O)_2$] complex.

3.1. Photoluminescent investigation

The luminescent doped polymer materials PA:(x%)Eu(tta) and PP/PA:(x%)$Eu(tta)_3$ exhibit highly intense red emission color under excitation with a UV light lamp (Fig. 5). As it can be seen, a high red emission intensity for the $[Eu(tta)_3(H_2O)_2]$ complex in powder form (a_1, a_2), PA:(5 %)$Eu(tta)_3$ film (Fig. 5b_1,b_2) and PA:(5 %)$Eu(tta)_3$ extruded forms (Fig. 5c_1, c_2). The indexes 1 refers to the samples under white light and 2 refers to samples under UV irradiation (at 360 nm).

The excitation spectra of the PA:(x%)$Eu(tta)_3$ and PP/PA:(x%)Eu $(tta)_3$ doped polymer films (x = 1, 5, and 10 %) were recorded at 298 K with emission monitored at 616 nm of the $^5D_0 \rightarrow {}^7F_2$ transition of Eu^{3+} ion, in the spectral range of 250–500 nm (Fig. 6). The high-intensity broad excitation bands centered at 350 nm are assigned to the allowed S_1–S_0 electronic transition originating from the tta ligand that overlaps with those from the PA and PP polymers. The excitation bands of the polymeric systems present similar spectral profiles, showing an increase in excitation intensities with an increase in the doping concentrations for both PA and PP/PA polymer systems. It is noteworthy that the main narrow excitation peak of the europium complex originated from the $^7F_0 \rightarrow {}^5D_2$ (464 nm) transition is not observed in the doped polymeric system (Fig. 6a and b). This result suggests that the intramolecular energy transfer is from organic moiety to Eu^{3+} ion [1–17,26]. On the other hand, Kumar et al. [27–29] reported the energy transfer process

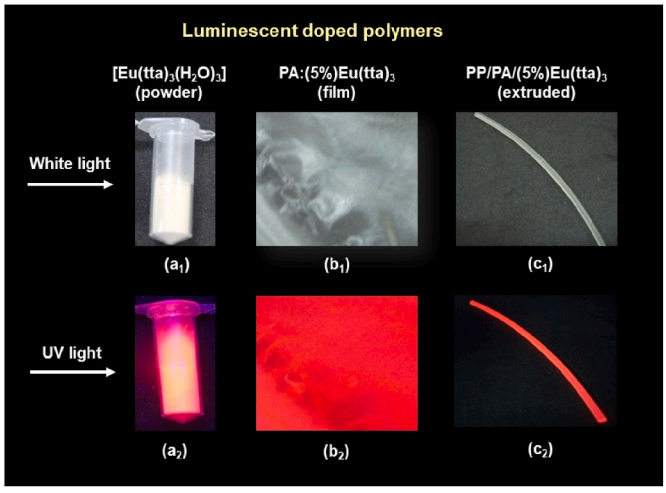

Fig. 5. Illustration of the luminescent materials, precursor Eu^{3+} complex (a_1 and a_2), PA:(5 %)$Eu(tta)_3$ films (b_1 and b_2) and PP:PA:(5 %)$Eu(tta)_3$ extruded form (c_1 and c_2). Indexes 1 and 2 refer to exposure to white light and under 350 nm irradiation, respectively. The photographs of the samples were taken with a digital camera.

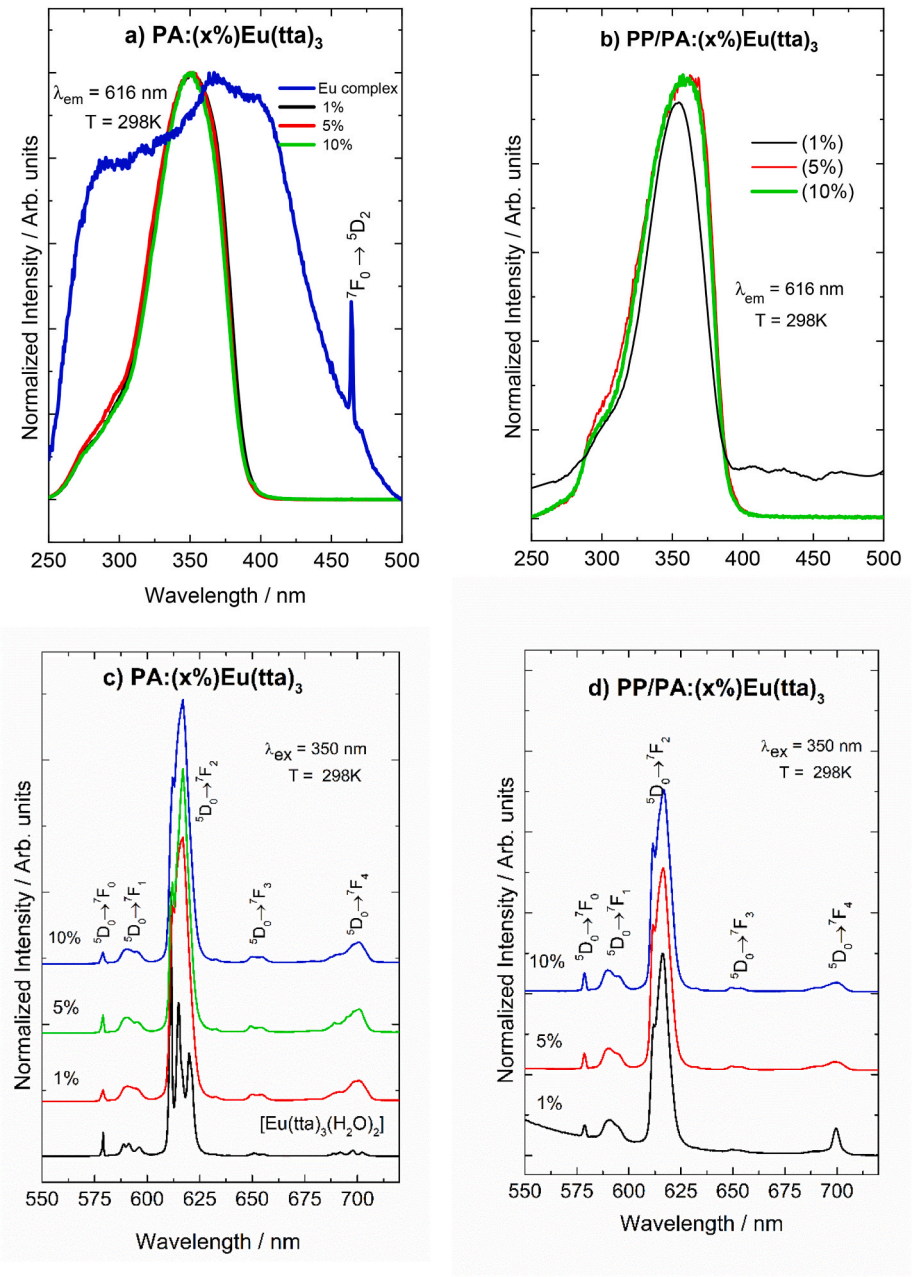

Fig. 6. Excitation spectra of the solid-state of the $Eu(tta)_3.(H_2O)_2$ (blue line in (a)) and the doped PA and PP/PA polymer films: a) PA:(x%)$Eu(tta)_3$, and b) PP/PA:(x %)$Eu(tta)_3$ at 1, 5, and 10 % concentrations. All spectra were recorded by monitoring the emission at the $^5D_0 \rightarrow {}^7F_2$ transition ($\lambda_{em.} = 616$ nm) of the Eu^{3+} ion. Emission spectra of the doped polymer films: a) PA:(x%)$Eu(tta)_3$, and $[Eu(tta)_3(H_2O)_2]$ (black line) and d) PP/PA:(x%)$Eu(tta)_3$ at 1, 5, and 10 %. All emission spectra were recorded under excitation at 350 nm.

between metal-metal ions.

The emission spectra of PA:(x%)$Eu(tta)_3$ and PA/PP:(x%)$Eu(tta)_3$ doped polymer systems (x = 1, 5, and 10 %) were recorded in the spectral range of 550–720 nm at 298 K, under excitation at 350 nm (Fig. 6c and d) show emission bands assigned to $^5D_0 \rightarrow {}^7F_{0\text{-}4}$ transitions of Eu^{3+} ion when compared to the $[Eu(tta)_3(H_2O)_2]$ precursor complex (Fig. 6c). The highest emission intensity peaks are assigned to the hypersensitive $^5D_0 \rightarrow {}^7F_2$ transition at 616 nm, suggesting that the europium ion occupies non-centrosymmetric sites for all doped polymer systems. The broad emission bands are due to the effect of the distribution of the multisites occupied by the Eu^{3+} ion in the polymeric system, producing an inhomogeneous line broadening in their emission bands [13,15,26, 30–35].

It is worth noting that a broad phosphorescence band attributed to the $T_1 \rightarrow S_0$ transition [36–39] of the tta ligand is absent in Fig. 6c and d. This optical feature indicates an efficient intramolecular energy transfer from the T_1 states of the tta ligand to the excited $^5D_1$ and $^5D_0$ levels of the Eu^{3+} ion.

When PP is doped with the PA:(x%)$Eu(tta)_3$ system (x = 1, 5, and 10 %), the resultant emission spectra showed the homogeneous dilution of the luminescent films in the polypropylene polymer (Fig. 6c and d). As a result, the dilution does not change the structure of PA:Eu(tta) once the spectra exhibited by PP/PAEu(tta) present the same emission profiles from the $^5D_0 \rightarrow {}^7F_{0\text{-}4}$ transitions. Accordingly, as PP polymer is a polyolefin with a saturated macrochain, the $[Eu(tta)_3(H_2O)_2]$ complex remains protected by the PA polymer acting as an optical marker and does not interact with PP polymer.

The luminescence decay curves of doped polymer films were

obtained with emission monitored at hypersensitive $^5D_0 \rightarrow {}^7F_2$ transition. The decay curves were adjusted with a first-order exponential decay function and the lifetime of the $^5D_0$ emitting level obtained from the decay curve of the doped blends and films are shown in Fig. S4 and Table 2. For the doped polymeric systems, it was observed a significant increase in lifetime compared to the precursor complex, suggesting the substitution of the water molecules in the Eu^{3+} complex for the polymeric groups.

Based on the emission spectra of the Eu^{3+} doped polymeric samples (Fig. 6c and d) were determined the experimental intensity parameters Ω_2 and Ω_4 by using the $^5D_0 \rightarrow {}^7F_2$ and $^5D_0 \rightarrow {}^7F_4$ transitions. Besides, the $^5D_0 \rightarrow {}^7F_1$ magnetic dipole-allowed transition is used as the reference. Therefore, the Ω_2 and Ω_4 parameters can be calculated according to Equation (1) [4,37,38]:

$$\Omega_\lambda = \frac{3\hbar c^3 A_{0\rightarrow\lambda}}{4e^2\omega^3\chi\langle {}^7F_\lambda \| U^{(\lambda)} \| {}^5D_0\rangle^2} \quad (1)$$

where ħ is Planck's constant divided by 2π, c is the speed of light and ω is the angular frequency of the transition. $\chi = n(n^2+2)^2/9$ is the Lorentz local field correction and n is the linear refractive index of the medium (n = 1.5 for this complex). The quantities $\langle {}^7F_\lambda \| U^{(\lambda)} \| {}^5D_0\rangle^2$ are the square reduced matrix elements, whose values are equal to 0.0032 and 0.0023 for λ = 2 and 4, respectively [38–43]. The $A_{0\rightarrow J}$ are spontaneous emission coefficients assigned to the $^5D_0 \rightarrow {}^7F_J$ transitions of the Eu^{3+} ion. The $^5D_0 \rightarrow {}^7F_1$ transition is governed practically by the magnetic dipole mechanism; therefore its spontaneous emission coefficient ($A_{0\rightarrow1}$) is mainly insensitive to the ligand field and it is taken as an internal standard. The spontaneous emission coefficients ($A_{0\rightarrow J}$) for the Eu^{3+} doped polymeric samples can be calculated by equation (2).

$$A_{0\rightarrow J} = \left(\frac{S_{0\rightarrow J}}{S_{0\rightarrow1}}\right) A_{0\rightarrow1} \quad (2)$$

where $S_{0\rightarrow J}$ and $S_{0\rightarrow1}$ are areas under emission curves from the $^5D_0 \rightarrow {}^7F_J$ (J = 2, 4, and 6) and $^5D_0 \rightarrow {}^7F_1$ transitions, respectively, and they are proportional to the number of the emitted photons [4,37]. The $^5D_0 \rightarrow {}^7F_6$ transition is usually not observed experimentally. Therefore, this transition is not considered in this work.

It is possible to calculate the total spontaneous emission for the emitting $^5D_0$ level. The radiative (A_{rad}) and non-radiative (A_{nrad}) decay processes and lifetime (τ) are correlated through equation (3) [4,37,40]:

$$A_{tot} = \frac{1}{\tau} = A_{rad} + A_{nrad} \quad (3)$$

where A_{rad} can be obtained by summing the radiative rates $A_{0\rightarrow J}$ for each $^5D_0 \rightarrow {}^7F_J$ transition by the expression $A_{rad} = \sum A_{0\rightarrow J}$. The intrinsic emission quantum yield (Q^{Eu}_{Eu}) of the $^5D_0$ emitting level of the Eu^{3+} ion is given by equation (4).

$$Q^{Eu}_{Eu} = \frac{A_{rad}}{A_{rad} + A_{nrad}} \quad (4)$$

The experimental intensity parameters Ω_2 and Ω_4 are very sensitive to the chemical environment around the Eu^{3+} ion and consider the simultaneous contributions from Forced Electric Dipole (FED) and Dynamic Coupling (DC) mechanisms. The Ω_2 intensity parameter is more influenced by small angular changes in the first coordination sphere. Therefore, the Ω_2 value is equal to zero when the europium ion is located in the center of symmetry, leading to the vanish of the emission band assigned to the $^5D_0 \rightarrow {}^7F_2$ transition for centrosymmetric systems. A point to be observed in Table 2 is that the polymeric systems present a lower value of the intensity parameter Ω_2 compared to the $[Eu(tta)_3(H_2O)_2]$ suggesting an angular distortion lower than the complex. In addition, when we compare the Ω_2 values between the PA:(x%)$Eu(tta)_3$ and PA/PP:(x%)$Eu(tta)_3$ polymer systems (x = 1, 5 and 10 %) it is observed that Ω_2 decreases with the inclusion of PP polymer, demonstrating a low distortion in the first coordination sphere due to a small hypersensitive character of $^5D_0 \rightarrow {}^7F_2$ transition, also indicating the noncentrosymmetric character.

The Ω_4 intensity parameter is more sensitive to lanthanide-ligating atom bond distances, therefore, giving information on the covalence. Table 2 shows that the Ω_4 values of the PA:(x%)$Eu(tta)_3$ are higher than for the Eu^{3+}-complex, suggesting the covalence of ligand-metal ion is more relevant for this doped film. Besides, the PP/PA:(x%)$Eu(tta)_3$ doped polymeric materials have the lowest Ω_4 values compared to the Eu-complex and PA:(x%)$Eu(tta)_3$, which indicate that the covalence of the metal ion–organic bonding is less relevant for this system (Table 2).

When taking into consideration the intrinsic emission quantum yield values of the PA:(x%)$Eu(tta)_3$ doped polymeric films ($Q^{Eu}_{Eu} \sim 53$ %) are higher than that of the europium complex (29 %) reported in Table 2. In addition, PA:(1 %)$Eu(tta)_3$ doped polymeric films have higher emission quantum yields (56 %) than those for poly(methyl methacrylate) PMMA:(1 %)$Eu(tta)_3$ materials ($Q^{Eu}_{Eu} \cong 45$ %) reported by Kai et al. [13,15,33]. Therefore, these photoluminescent data indicate that the PP polymeric matrix also acts as an efficient sensitizer in the energy transfer from the organic moiety to the Eu^{3+} ion. Besides, the optical results show that a saturation effect occurred at 1 % of the europium complex mass concentration of PA:$Eu(tta)_3$ system (36 %). On the other hand, The Q^{Eu}_{Eu} values of the extruded PP/PA:(x%)$Eu(tta)_3$ doped system are lower 23 % (x = 5) and 24 %, (x = 10) related to that $[Eu(tta)_3(H_2O)_2]$ complex ($Q^{Ln}_{Ln} = 29$ %), suggesting a quite similar luminescent behavior.

The CIE chromaticity diagram (*Commission Internationale de l'Éclairage*) was used to show the gradual spectral shifting of the PA and PP/PA doped luminescent polymeric materials in comparison to the precursor Eu^{3+} complex [39–44]. The coordinates (x,y) are calculated considering the emission spectra profiles and relative intensities of each luminescent material (Fig. 7 Table S3).

The CIE color coordinates (x, y), color rendering index CRI(Ra), and correlated color temperature (CCT) values were calculated for the PA:(x%)[Eu(tta) and PP/PA:Eu(tta)x% polymer films and are given in Table S3. CCT values signify the emergence of light as cool or warm. Usually, it is well-known that light with CCT <3200 K emits warm light while those with CCT >4000 K are given cool white light [44]. In this work, it was observed CCT values for the doped polymer samples lower than 3200 K, which indicated warm light. It was noticed that the (x,y) values are positioned in the reddish region equivalent to $^5D_0 \rightarrow {}^7F_2$ (617 nm) electronic transition, suggesting that these luminescent polymeric

Table 2
Experimental values of intensity parameters (Ω_2, Ω_4), determined from the $^5D_0 \rightarrow {}^7F_2$ and $^5D_0 \rightarrow {}^7F_4$ transitions based on the emission spectra (298 K) of the Eu^{3+} complexes and doped polymeric materials PA:$[Eu(tta)_3(H_2O)_2]$x% and PP/PA:$[Eu(tta)_3(H_2O)_2]$x% (where x = 1, 5 and 10) and A_{rad}, A_{nrad}, A_{tot}, Q^{Ln}_{Ln} and τ.

Sample	Ω_2 (10^{-20}cm^2)	Ω_4 (10^{-20}cm^2)	A_{rad} (s^{-1})	A_{nrad} (s^{-1})	τ (ms)	A_{tot} (s^{-1})	Q^{Ln}_{Ln} (%)
$[Eu(tta)_3(H_2O)_2]$	33.0	4.6	923	2923	0.26	3846	29
PA:(1 %)$Eu(tta)_3$	26.1	6.2	921	718	0.61	1639	56
PA:(5 %)$Eu(tta)_3$	23.6	6.8	856	927	0.56	1785	48
PA:(10 %)$Eu(tta)_3$	26.4	6.5	937	730	0.60	1667	56
PP/PA:(1 %)$Eu(tta)_3$	20.8	3.7	731	1315	0.49	2046	36
PP/PA:(5 %)$Eu(tta)_3$	14.9	1.8	523	1628	0.46	2151	24
PP/PA:(10 %)$Eu(tta)_3$	15.5	1.9	543	1727	0.44	2270	23

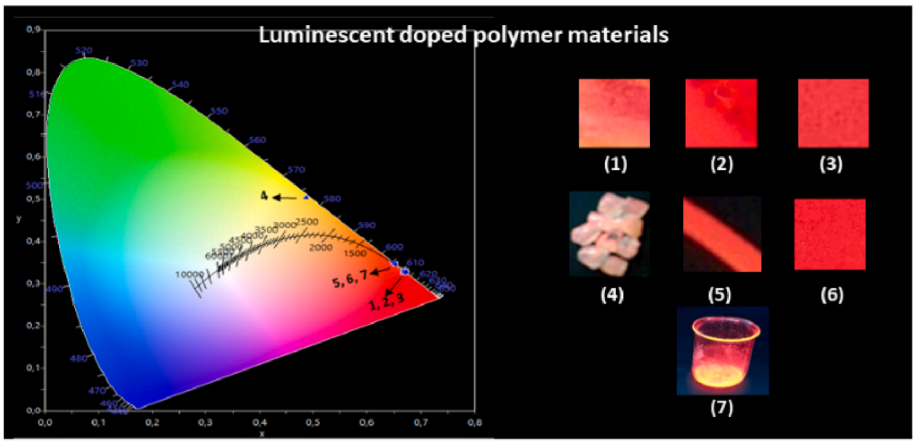

Fig. 7. CIE chromaticity diagram showing, at left, the emission color tuning of PA:(x%)[Eu(tta) for x = 1 % (1), 5 % (2), 10 % (3) and PP/PA: Eu(tta)x%, x = 1 % pellets (4), 5 % extruded (5), 10 % film (6), and $[Eu(tta)_3(H_2O)_2]$ complex in powder (7). The photographs of polymeric films and the complex taken with a digital camera show their reddish emissions under UV irradiation at 350 nm (right side).

materials are relevant for promoting reddish lighting devices. The color rendering index (CRI) indicates the extent of a light source's color rendering properties. CRI indicates how well the light source reproduces colors.

4. Conclusion

PA:(x%)$Eu(tta)_3$ doped polymeric films and PP/PA:(x%)$Eu(tta)_3$ extruded form samples (x = 1, 5 and 10 %) were successfully produced. TG data of all doped systems indicated that the precursor Eu^{3+}-complex was immobilized in the PA polymeric matrix via Eu–O interaction. The DSC data of the extruded samples indicate that the PP/PA:(x%)$Eu(tta)_3$ system is more favorable for the extrusion process conditions and a more economic advantages. The polymer matrix brought higher thermal stability to the Eu^{3+} complex. The PA tag when tested for polypropylene (PP), one polyolefin without heteroatoms to allow good luminescent material resulted in perfect dispersion.

The emission spectral data show that the PP extruded with the PA:(x %)$Eu(tta)_3$ tag conserves the luminescence features and presents high emission quantum yield values and all these polymeric materials exhibit a high red emission intensity. The Q_{Eu}^{Eu} values of the PA:(x%)$Eu(tta)_3$ doped polymeric films are higher than that from the Eu^{3+} complex making them suitable for utilization as light-converting molecular devices. In addition, photoluminescent data indicate that the PP polymeric matrix also acts as an efficient sensitizer in the energy transfer from the organic moiety to the Eu^{3+} ion of the PA-tagged. This optical property was promoted by PP encapsulation and contributes to the high luminescent stability of the film under processing.

CRediT authorship contribution statement

D.F. Parra: Conceptualization, Funding acquisition, Investigation, Writing – original draft. **L.G. Marchini:** Formal analysis, Methodology. **M.C.F.C. Felinto:** Data curation, Writing – review & editing. **H.F. Brito:** Data curation, Supervision, Writing – review & editing.

Declaration of competing interest

The authors declare that they have no known competing financial interests or personal relationships that could have appeared to influence the work reported in this paper.

Data availability

Data will be made available on request.

Acknowledgments

The authors thank CNPQ for Leonardo Marchini's MS grant. D.F.P. thanks to CNPQ (N 310202/2022–1) and the Multiuser Laboratory of Advanced Optical Spectroscopy - LMEOA, of the Chemistry Institute of UNICAMP - Campinas, São Paulo, and CNEN. Besides, H.F.B., D.F.P. and M.C.F.C.F. authors are grateful to FAPESP (No 2021/08111–2) and CNPq (No. 308872/2022–3 and 314032/2021/5) for the financial support.

Appendix A. Supplementary data

Supplementary data to this article can be found online at https://doi.org/10.1016/j.optmat.2024.115396.

References

[1] J.-C.G. Bunzli, On the design of highly luminescent lanthanide complexes, Coord. Chem. Rev. 293 (2015) 19.
[2] K. Binnemans, Lanthanide-based luminescent hybrid materials, Chem. Rev. 109 (2009) 4283.
[3] H.F. Brito, O.L. Malta, M.C.F.C. Felinto, E.E.S. Teotonio, Patai series, in: By J. Zabicky (Ed.), The Chemistry of Metal Enolates, John Wiley & Sons Ltd., New Jersey, 2009, p. 131.
[4] A.N. Carneiro Neto, E.E.S. Teotonio, G.F. de Sá, H.F. Brito, J. Legendziewicz, L. D. Carlos, M.C.F.C. Felinto, P. Gawryszewska, R.T. Moura Jr., R.L. Longo, W. M. Faustino, O.L. Malta, Modeling intramolecular energy transfer in lanthanide chelates: a critical review and recent advances, North-Holland, in: J.-C. Bunzli, V. Pecharsky (Eds.), Handbook on the Physics and Chemistry of Rare Earths, first ed., 2019, p. 56. chap. 310) 56.
[5] P. Tanner, L. Zhou, C. Duan, K.L. Wong, Misconceptions in electronic energy transfer: bridging the gap between chemistry and physics, Chem. Soc. Rev. 47 (2018) 5234.
[6] I.F. Costa, L. Blois, T.B. Paolini, I.P. Assunção, E.E.S. Teotonio, M.C.F.C. Felinto, R. T. Moura Jr., R.L. Longo, W.M. Faustino, L.D. Carlos, O.L. Malta, A.N. Carneiro Neto, H.F. Brito, Luminescence properties of lanthanide tetrakis complexes as molecular light emitters, Coord. Chem. Rev. 502 (2024) 215590.
[7] K. Binnemans, Interpretation of europium(III) spectra, Coord. Chem. Rev. 295 (2015) 1.
[8] L.D. Carlos, R.A.S. Ferreira, V. de Zea Bermudez, S.J.L. Ribeiro, Lanthanide-containing light-emitting organic–Inorganic hybrids: a bet on the future, Adv. Mater. 21 (2009) 509.
[9] Y.M. Fadieiev, S.S. Smola, E.V. Malinka, N.V. Rusakova, Study of association of Eu (III) β-diketonate-1,10-phenanthroline complexes in silica-based hybrid materials, J. Lumin. 183 (2017) 121.
[10] T.V.U. Gangan, S. Sreenadh, M.L.P. Reddy, Visible-light excitable highly luminescent molecular plastic materials derived from Eu^{3+}-biphenyl based β-diketonate ternary complex and poly(methylmethacrylate), J. Photochem. Photobiol., A 328 (8) (2016) 171.
[11] C. Yang, H. Zhou, J. Xu, Y. Li, M. Lu, J. He, Q. Zhang, A series of highly quantum efficiency PMMA luminescent films doped with Eu-complex as promising light-conversion molecular devices, J. Mater. Sci. Mater. Electron. 27 (2016) 11284.

[12] W. Li, Y. Tao, G. An, P. Yan, Y. Li, G. Li, One-dimensional luminescent composite nanofibers of Eu(TFI)$_3$TPPO/PVP prepared by electrospinning, Dyes Pigments 146 (2017) 47.

[13] J. Kai, D.F. Parra, H.F. Brito, Polymer matrix sensitizing effect on photoluminescence properties of Eu^{3+}–β–diketonate complex doped into poly–3–hydroxybutyrate (PHB) in film form, J. Mater. Chem. 18 (2008) 4549.

[14] J.D. Shin, W.J. Lim, K.S. Yu, J.H. Lee, N.S. Lee, Y.G. Jeong, S.-Y. Han, D.K. Kim, Luminescent polystyrene latex nanoparticles doped with β-diketone europium chelate and methacrylic acid, Eur. Polym. J. 83 (2016) 89.

[15] J. Kai, M.C.F.C. Felinto, L.A.O. Nunes, O.L. Malta, H.F. Brito, Intermolecular energy transfer and photostability of luminescence-tunable multicolor PMMA films doped with lanthanide β-diketonate complexes, J. Mater. Chem. 21 (2011) 3796.

[16] T.M. George, M.J. Sajan, N. Gopakumar, M.L.P. Reddy, Bright red luminescence and triboluminescence from PMMA-doped polymer film materials supported by Eu^{3+}-triphenylphosphine based β-diketonate and 4,5-bis(diphenylphosphino)-9,9-dimethylxanthene oxide, J. Photochem. Photobiol., A 317 (15) (2016) 88.

[17] H.F. Brito, O.L. Malta, J.F.S. Menezes, Luminescent properties of diketonates of trivalent europium with dimethyl sulfoxide, J. Alloys Compd. 336 (2000) 303.

[18] D.F. Parra, P.L. Forster, R. Lyszczek, Thermal behavior of the highly luminescent poly(3-hydroxybutyrate):Eu(tta)3(H2O)2 red-emissive complex, J. Therm. Anal. Calorimetry 114 (2013) 1049.

[19] D.F. Parra, A. Mucciolo, H.F. Brito, L.C. Thompson, Optical characteristics of the Eu^{3+}–beta-diketonate complex doped into epoxy resin, J. Solid State Chem. 171 (2003) 412.

[20] K. Zarshenas, A. Raisi, A. Aroujaliana, Surface modification of polyamide composite membranes by corona air plasma for gas separation applications, RSC Adv. 5 (2015) 19760.

[21] C. Gabelich, J.C. Frankin, F.W. Gerringer, K.P. Ishida, I.H. Suffet, Enhanced oxidation of polyamide membranes using monochloramine and ferrous iron, J. Membr. Sci. 258 (2005) 64.

[22] L. Ji, G. Su, Q. Yuan, X. Zhang, T. Zhou, Difference in the micro-dynamics mechanism between aromatic nylon and aliphatic nylon during water absorption: spectroscopic evidence, Phys. Chem. Chem. Phys. 20 (2018) 26764.

[23] L. Marchini, Development of optical marker for polyolefin processing, in: Dissertation Presented at IPEN- Nuclear Technology - Materials, São Paulo, Brazil, 2013.

[24] L. Peng, J. Li, S. Peng, C. Yi, F. Jiang, The crystal-form transition behaviours and morphology changes in a polyamide 6 cyclic dimer, R. Soc. Open Sci. 5 (2018) 180957.

[25] K. Binnemans, Rare-earth beta-diketonates, in: K.A. Gschneidner Jean-Claude, G. Bunzli, Vitalij K. Pecharsky (Eds.), Handbook on the Physics and Chemistry of Rare Earths, vol. 35, Elsevier 1st Edition, 2005, p. 35.

[26] L.D. Carlos, Y. Messaddeq, H.F. Brito, R.A. Sá Ferreira, V. Zea Bermudez, S.J. L. Ribeiro, Full-color phosphors from europium(III)-Based organosilicates, Adv. Math. 12 (2000) 594.

[27] K.N. Kumar, K. Sivaiah, S. Buddhudu, Structural, thermal and optical properties of Tb^{3+}, Eu^{3+} and co-doped (Tb^{3+}+Eu^{3+}): PEO+PVP polymer films, J. Lumin. 147 (2014) 316.

[28] K.N. Kumar, L. Vijayalakshmi, J.S. Kim, J. Shim, M. Cho, M. Kang, B.K. Gupta, Energy transfer (In^{3+} → Eu^{3+}) based Polyvinyl Alcohol polymer composites for bright red luminescence, Opt. Mater. 70 (2017) 41.

[29] K.N. Kumar, L. Vijayalakshmi, Y.C. Ratnakaram, Energy transfer based photoluminescence properties of (Sm^{3+}+Eu^{3+}):PEO+PVP polymer films for Red luminescent display device applications, Opt. Mater. 45 (2015) 148.

[30] P. Miluski, M. Kochanowicz, J. Zmojda, D. Dorosz, Properties of Eu doped poly (methyl methacrylate) optical fiber, Opt. Eng. 56 (2017), 027106-5.

[31] O.L. Malta, M.A. Couto dos Santos, L.C. Thompson, N.K. Ito, Intensity parameters of 4f-4f transitions in the Eu(dipivaloylmethanate)$_3$ 1,l0-phenanthroline complex, J. Lumin. 69 (1996) 77.

[32] S. Biju, R.O. Freire, R. Scopelliti, J.-C.G. Bünzli, H.K. Kim, An Eu(III) tetrakis (β-diketonate) dimeric complex: photophysical properties, structural elucidation by sparkle/AM1 calculations, and doping into PMMA films and nanowires, Inorg. Chem. 53 (2014) 8407.

[33] E.B. Gibelli, J. Kai, E.E.S. Teotonio, O.L. Malta, M.C.F.C. Felinto, H.F. Brito, Photoluminescent PMMA polymer films doped with Eu^{3+}-β-diketonate crown ether complex, J. Photochem. Photobiol., A 251 (2013) 154.

[34] L.H.C. Francisco, M.C.F.C. Felinto, H.F. Brito, E.E.S. Teotonio, O.L. Malta, Development of highly luminescent PMMA films doped with Eu^{3+} β-diketonate coordinated on the ancillary ligand, J. Mater. Sci. Mater. Electron. 30 (2019) 16922.

[35] F.P. Aguia, I.F. Costa, J.G.P. Espínola, W.M. Faustino, J.L. Moura, H.F. Brito, T. B. Paolini, M.C.F.C. Felinto, E.E.S. Teotonio, Luminescent hybrid materials functionalized with lanthanide ethylenodiaminotetraacetate complexes containing β-diketonate as antenna ligands, J. Lumin. 170 (2016) 538.

[36] O.L. Malta, H.F. Brito, J.F.S. Menezes, F.R.G. Silva, J.R. Alves, S.F.S. Farias, A.V. M. Andrade, Spectroscopic properties of a new light-converting device: Eu (thenoyltrifluoroacetonate)$_3$2(dibenzyl sulfoxide). A theoretical analysis based on structural data obtained from a sparkle model, J. Lumin. 75 (1997) 255.

[37] G.F. de Sá, O.L. Malta, M.C. Donega, A.M. Simas, R.L. Longo, P.A. Santa-Cruz, E. F. Silva Jr., Spectroscopic properties and design of highly luminescent lanthanide coordination complexes, Coord. Chem. Rev. 196 (2000) 165.

[38] W.T. Carnall, H. Crosswhite, H.M. Crosswhite, Energy Structure and Transition Probabilities of the Trivalent Lanthanides in LaF_3, Argonne National Laboratory Report, unnumbered, 1977.

[39] X. Huang, H. Guo, B. Li, Eu^{3+}-activated $Na_2Gd(PO_4)(MoO_4)$: a novel high-brightness red-emitting phosphor with high color purity and quantum efficiency for white light-emitting diodes, J. Alloys Compd. 720 (5) (2017) 29.

[40] J.Y. Park, J.W. Chung, H.K. Yang, Versatile fluorescent Gd_2MoO_6:Eu^{3+} nanophosphor for latent fingerprints and anti-counterfeiting applications, Ceram. Int. 45 (2019) 11591.

[41] H.-W. Tseng, W.-C. Tzou, S. We, P.-Y. Lin, C.-F. Yang, Rapid ultrasonic-microwave assisted synthesis of Eu $^{3+}$ doped Y_2O_3 nanophosphors with enhanced luminescence properties, J. Mater. Res. Technol. 9 (6) (2020) 14051.

[42] John Selverian, OSRAM ColorCalculator Software, 2017.

[43] K.P. Mani, V. George, I.M. Abraham, Synthesis and photoluminescence studies of one dimensional Sm2MoO6 nanofibers derived from electrospinning process, J. Mater. Res. Technol. 4 (2) (2015) 224.

[44] K. Sivaiah, S. Buddhudu, Photoluminescence spectra of Sm^{3+} and Dy^{3+}:PVP polymer films, Indian J. Phys. 86 (12) (2012) 1079.